Acta Cryst. (1981). B**37**, 1803–1807

The Structure of TiNi Martensite

BY G. M. MICHAL* AND R. SINCLAIR

Department of Materials Science and Engineering, Stanford University, Stanford, California 94305, *USA*

(*Received* 22 *May* 1980; *accepted* 23 *March* 1981)

Abstract

The crystal structure of the martensite (low-temperature) phase of the intermetallic compound TiNi has been determined based upon single-crystal electron and powder X-ray diffraction data. The structure is monoclinic, $P112_1/m$, with dimensions $a = 2{\cdot}885$ (4), $b = 4{\cdot}622$ (5), $c = 4{\cdot}120$ (5) Å and $\gamma = 96{\cdot}8$ (1·0)°. The atomic positions were determined by considering the collapse of the high-temperature structure occurring by a shuffle of its {110} planes, taking into account the constraints imposed by the difference in size of the Ti and Ni atoms. The final structure yielded an R of 0·17 for the first 22 reflections and contains a set of interatomic bond lengths commensurate with those observed in other structures in the Ti–Ni system.

Introduction

The structures and transformation behavior responsible for the memory and superelastic effects in TiNi have been a source of speculation and confusion since the alloy's inception in the early 1960's. The basis of its unusual mechanical properties is now accepted to be a martensitic phase transformation from a high-temperature CsCl ($B2$) structure to one of lower symmetry. The crystal structure of the low-temperature, martensite phase is probably the most controversial topic concerning this intermetallic compound. The only universal agreement among the nine or more research groups who have worked on the martensite structure is that it may be described by a stacking sequence of prior $\{110\}_{B2}$ planes. The majority of the proposed structures are based upon a two-layer sequence. However, at least two reports (Gupta, 1972; Gupta, Johnson & Mukherjee, 1973; Nagasawa, 1971) of more complex stacking sequences have been made on specially heat-treated, thin-foil specimens using transmission electron microscopy (TEM).

When one reviews previous work on the martensite structure (Otsuka, Sawamura & Shimizu, 1971; Sandrock, 1971; Hehemann & Sandrock, 1971; Vatanayon & Hehemann, 1975; Marcinkowski, Sastri & Koskimaki, 1968; Mohamed, 1976; Mohamed & Washburn, 1977; Gupta, 1972; Gupta & Johnson, 1973; Dautovich & Purdy, 1965; Larson, 1979), it is clear that, although interpretations vary, there is a commonly quoted set of lattice constants. This structure can be interpreted as a monoclinic distortion of either the h.c.p. ($A3$) or AuCd ($B19$) structures. The agreement among the researchers who have performed refinements of the lattice constants is really quite good (Otsuka *et al.*, 1971; Hehemann & Sandrock, 1971). However, the controversy lies in the type of atomic shuffle occurring during the transformation and the orientation of that shuffle with respect to the lattice axes (*i.e.* where the atoms lie in the unit cell). None of the proposed combinations of axes and shuffles exhibit a reasonable set of interatomic bond lengths nor are they able to account for the basic intensity distributions of the commonly observed X-ray and electron diffraction data. For these reasons, the purpose of this paper is to present a new set of atomic coordinates for the martensite phase which is able to account for the observed diffraction data while maintaining bond lengths consistent with other well established structures in the Ti–Ni binary system. Clearly, for a complete understanding of the mechanism of the phase transformation and its associated macroscopic behavior, it is important to know the crystal structures of the phases involved.

Experimental

All alloy data presented in this report are from a composition 50·0 ± 0·1 at.% Ni, balance Ti. Single-crystal electron diffraction patterns were obtained from hot-rolled material annealed at 973 K for 41 h, then jet-electropolished to thin-foil form. Details of the experimental procedures are given elsewhere (Michal, 1979). The X-ray and neutron diffractometry data are taken from the work of Wang, Pickart & Alperin (1972), which represents the only presently published diffractometry scans from a TiNi martensite powder specimen (due to the difficulty in producing martensite

---

* Present address: The Republic Steel Research Center, 6801 Brecksville Road, Independence, Ohio 44131, USA.

0567-7408/81/101803-05$01.00

from TiNi powder). All other results are from sheet samples.

The martensite variant size is generally much smaller than the smallest feasible selected area aperture in the TEM, but on occasion a variant would be found large enough to obtain single-crystal patterns. The data obtained in this study are similar to those of previous workers, being indexed according to a single monoclinic phase. No long-period stacking-sequence structure was found. The lattice parameters are almost identical to those reported previously. Some additional reciprocal-lattice sections were also obtained. A complete catalogue of these results is presented by Michal (1979) and only those of critical importance are discussed here. More complex patterns, from several variants, can also be indexed completely using the same unique crystal structure (Michal, 1979).

Structure determination

After consideration of the previously proposed structures for the martensite phase in TiNi, those suggested by Otsuka *et al.* (1971) (OSS) and Hehemann & Sandrock (1971) (HS) (later modified by Vatanayon & Hehemann, 1975) were chosen for detailed study. These are representative of the two basic types of atomic shuffles proposed for all the monoclinic structures, as well as being the result of extensive efforts to determine the crystal structure using combined X-ray and TEM techniques. They are identical except for the orientation and magnitude of the atomic shuffle necessary for atoms in the *B*2 structure to reach their final positions in the martensite. The relevant crystallographic data for each are presented in Table 1. The predicted relative intensities of Cu *Kα* X-ray diffractometer peaks were computed by taking the product of the structure factor, its complex conjugate, the multiplicity, the Lorentz–polarization factor and a proportionality constant. Table 2 compares the calculated results for the first 22 *d*-spacings with the observed intensities from the diffractometer scan of Wang *et al.* (1972). Both sets of calculated intensities have major disagreements with the observed data.

The number of peaks which disagree by more than an order of magnitude with the experimental observations is five and three respectively for the OSS and HS structures. A more fundamental disagreement is found between these structures and the observed single-crystal Laue-zone electron diffraction patterns shown in Fig. 1. Because the 010, $1\bar{1}0$ and 110 reflections have a zero structure factor in the OSS structure every alternate row of spots in the pattern shown in Fig. 1(*a*) should not appear, even allowing for double diffraction. For the HS structure, the zero structure factor for the 001 and 101 reflections would predict that every alternate row of spots shown in Fig. 1(*b*) should be

Table 1. *Crystallographic data on proposed* TiNi *martensite structures*

Structure		HS*	Present	OSS†
System		Monoclinic	Monoclinic	Monoclinic
Space group		$P112_1/m$	$P112_1/m$	$P12/c1$
a (Å)		2·883	2·885	2·889
b (Å)		4·623	4·622	4·120
c (Å)		4·117	4·120	4·622
β (°)				96·8
γ (°)		96·8	96·8	
Atoms per unit cell		4	4	4
Positions of atoms				
(f)				$\frac{1}{2}y\frac{1}{4}, \frac{1}{2}\bar{y}\frac{3}{4}$ 2Ni: $y = 0·167$
(e)		$xy\frac{1}{4}, xy\frac{3}{4}$ 2Ti: $x = 0·5$ $y = 0·3125$ 2Ni: $x = 0·0$ $y = 0·1875$	$xy\frac{1}{4}, \bar{x}\bar{y}\frac{3}{4}$ 2Ti: $x = 0·5274$ $y = 0·279$ 2Ni: $x = 0·0525$ $y = 0·193$	$0y\frac{1}{4}, 0\bar{y}\frac{3}{4}$ 2Ti: $y = 0·333$
Conventional coordinates	Ti:	000 $0\frac{5}{8}\frac{1}{2}$	000 0·055, 0·558, $\frac{1}{2}$	000 $0\frac{1}{2}\frac{1}{2}$
	Ni:	$\frac{1}{2}\frac{1}{2}0$ $\frac{1}{2}\frac{1}{8}\frac{1}{2}$	0·580, 0·472, 0 0·475, 0·086, $\frac{1}{2}$	$\frac{1}{2}\frac{1}{2}0$ $\frac{1}{2}\frac{1}{6}\frac{1}{2}$
Bond lengths (Å)				
Ti–Ti		2·692 (2) 2·883 (2)	2·885 (2) 2·919 (2)	2·688 (2) 2·889 (2)
Ti–Ni		2·541 (2) 2·570 (2) 2·618 (2) 2·865 (2)	2·480 (2) 2·587 (1) 2·593 (1) 2·615 (2) 2·618 (1) 3·118 (1)	2·516 (4) 2·665 (2) 2.947 (2)
Ni–Ni		2·692 (2) 2·883 (2)	2·719 (2) 2·885 (2)	2·688 (2) 2·889 (2)

* Hehemann & Sandrock (1971).
† Otsuka, Sawamura & Shimizu (1971).

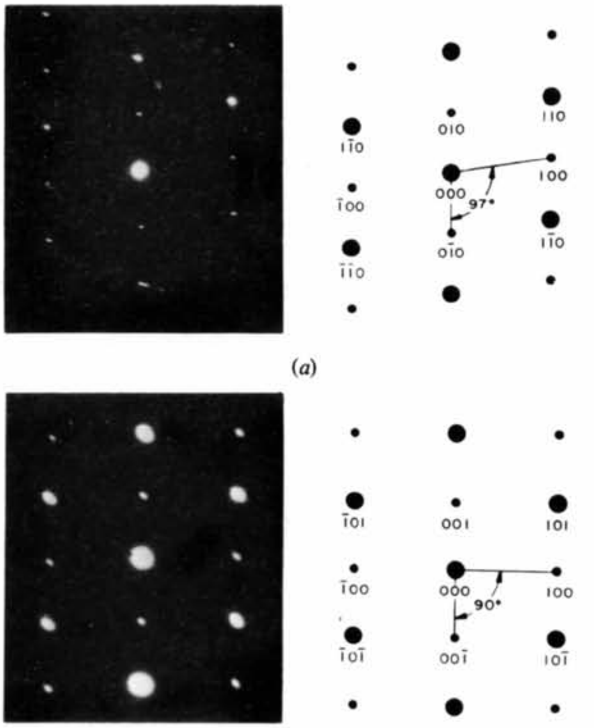

(*a*)

(*b*)

Fig. 1. Single-crystal Laue-zone patterns of the martensite phase. (*a*) A $[001]_M$ zone orientation (present work), (*b*) a $[010]_M$ zone orientation [after Otsuka *et al.* (1971)].

Table 2. *Comparison of calculated peak intensities for various* TiNi *structures with observed intensities from a powder specimen*

		X-rays				Neutrons	
		Present structure	Powder (Wang *et al.*)	OSS structure	HS structure	Powder (Wang *et al.*)	Present structure
h k l	*d* (Å)	I_{calc}	I_{obs}	I_{calc}	I_{calc}	I_{obs}	I_{calc}
0 1 0	4·590	5·5	5·5	0·0	0·4	12·7	12·5
0 0 1	4·120	0·0		0·7	0·0		0·0
0 1 1	3·066	1·4		2·0	2·0	100·0	100·0
1 0 0	2·865	0·7		1·1	1·0	25·1	43·8
$1\ \bar{1}\ 0$	2·570	13·0	9·7	0·0	14·3	4·1	8·5
1 0 1	2·352	10·6	13·8	42·4	0·0	17·9	2·5
1 1 0	2·311	2·4	42·1	0·0	10·3	9·7	0·1
0 2 0	2·295	53·6		78·5	34·5		3·3
$1\ \bar{1}\ 1$	2·181	100·0	100·0	100·0	100·0	9·7	5·7
0 0 2	2·060	53·8	50·0	13·8	48·6		5·7
1 1 1	2·016	94·3	94·7	77·1	77·1	12·7	11·5
0 2 1	2·005	26·4		0·2	44·3		6·9
$1\ \bar{2}\ 0$	1·904	1·4		0·3	0·2	6·6	7·2
0 1 2	1·879	0·9		60·6	0·1	6·6	3·4
$1\ \bar{2}\ 1$	1·728	8·3	7·9	15·0	0·2	11·8	14·4
1 2 0	1·696	0·3		0·2	0·1		11·7
1 0 2	1·673	0·3		0·1	0·4	19·7	24·9
$1\ \bar{1}\ 2$	1·607	5·3	7·9	0·3	5·9	2·6	5·6
1 2 1	1·568	0·1		10·4	0·1		3·9
1 1 2	1·538	1·2	18·4	0·2	5·0	6·5	0·1
0 2 2	1·533	26·1		9·5	16·7		2·5
0 3 0	1·530	1·0		0·0	0·1	6·5	6·8
		$R = 0{\cdot}17$		$R = 0{\cdot}65$	$R = 0{\cdot}19$		$R = 0{\cdot}37$

Note: Miller indices are for the present and HS structures. Indices for the OSS structure may be found by inverting the *b* and *c* axes.

absent. A final shortcoming of the previous structures is that they both require the Ti—Ti bond length to be as short as 2·69 Å. This value is thought to be unreasonably low when one considers that the Ti—Ti bond length observed in elemental Ti, in Ti_2Ni, $TiNi_3$ and in the high-temperature form of TiNi is never less than 2·89 Å (Michal, 1979).

In proposing a more reliable structure, the HS form was considered to be closer for two principal reasons. Firstly, the HS structure exhibits better agreement with the powder data than OSS, as evidenced by the much lower *R* factor shown in Table 2. Secondly, HS has the *B*2 phase collapsing along a direction normal to the atomic shuffle. This is consistent with the model originally proposed by Zener (1947) for the transition from a b.c.c. to a closer packed structure. OSS has the *B*2 structure expanding along a direction normal to the atomic shuffle, which does not normally occur in this type of (β phase) martensitic reaction.

The HS structure is simply a monoclinic distortion of the orthorhombic *B*19 structure, the classic example of which is the martensitic phase (β') in near equiatomic AuCd (Ölander, 1932) often discussed as analogous to the TiNi martensite phase. Therefore, some of the crystallographic features in the Au—Cd system were examined as possible pointers for solving the present structure. The similarities between the two systems are quite striking. In both, the smaller species has a f.c.c. structure and the larger an h.c.p. structure, in their elemental states. Also, the martensite phases are formed from a *B*2 structure. The major difference is the atomic-radius ratio, r_1/r_2, between the atoms in each system (*International Tables for X-ray Crystallography*, 1968). For Au—Cd the ratio is 0·97, while in Ti—Ni it is 0·86.

When Zener (1947) first considered the shuffles associated with the collapse of a b.c.c. type structure, the possible influence of a difference in atomic size in a *B*2 structure was not directly taken into account. The magnitude of the $\langle 110\rangle_{B2}$ shuffle is one eighth when the atomic-radius ratio is unity. If the ratio is less than unity, the magnitude of the shuffle must be smaller. When the ratio falls to the value of the ideal CsCl structure, 0·73, the magnitude of the shuffle is reduced to zero. This is because the large atoms are already touching along $\langle 100\rangle_{B2}$-type directions in that structure. An expression for the magnitude *X* of the $\langle 110\rangle_{B2}$ shuffle as a function of the atomic-radius ratio in the range $0{\cdot}73 \le r_1/r_2 \le 1$ is as follows

$$X = \tfrac{1}{2}\left\{1 - \frac{3}{(1 + r_1/r_2)^2}\right\}. \qquad (1)$$

In the AuCd β' phase, the $\frac{1}{8}\langle 110\rangle_{B2}$ shuffle reduces the Cd—Cd bond length to 2·994 Å which is effectively equal to the value in the elemental state. The 0·125 magnitude of the shuffle is in close agreement with the value of 0·114 calculated using equation (1). When the radius ratio for Ti—Ni is considered, through equation (1), the magnitude of the predicted shuffle is $0{\cdot}066\langle 110\rangle_{B2}$ which is approximately equal to $0{\cdot}06\langle 010\rangle_M$ using the martensite-phase lattice coordinates.

The first difference between the *B*19 structure and the TiNi martensite structure then is that the magnitude of the shuffle is about one half as great in TiNi due to the large difference in the size of the atoms. The second difference is due to the monoclinic distortion of the unit cell present in the TiNi martensite phase. This distortion causes a difference in the Ti—Ni bond lengths along the two diagonals in the plane of the shuffle, corresponding to the basal plane of the martensite unit cell. After the homogeneous shuffle of $0{\cdot}06\langle 010\rangle_M$, as shown in Fig. 2, there is room for the atoms to resettle in the general direction of the longer diagonal of the basal plane. This would happen in order to maximize the number of bond lengths close to those that would occur if the atoms had their elemental atomic radii. This resettling process is shown schematically in Fig. 3.

The concepts of a homogeneous shuffle followed by a slight resettling of the atoms are central to the point of view used in the present structure determination. Firstly, the atomic coordinates were determined after a homogeneous shuffle of $0{\cdot}06\langle 010\rangle_M$. Secondly, the atoms were allowed to move slightly from these positions in such a way as to remain in the (*e*) positions of the $P112_1/m$ space group. This was chosen because it was the monoclinic space group with the highest symmetry consistent with a systematic absence of reflections of the type 00*n*, where *n* is an odd integer. The general directions and magnitudes of the resettling motions were determined considering two factors: first, to establish certain bond lengths among the final atom positions and, secondly, to optimize the fit between the calculated and observed electron and X-ray diffraction data. The atoms were moved repeatedly while those bond lengths were maintained and after each perturbation the peak intensities for the first 30 *d*-spacings were computed and compared with the available diffraction data. This process was continued until the best fit was obtained. The crystallographic data for this structure and the intensities computed for the first 22 X-ray diffraction peaks are also presented in Tables 1 and 2.

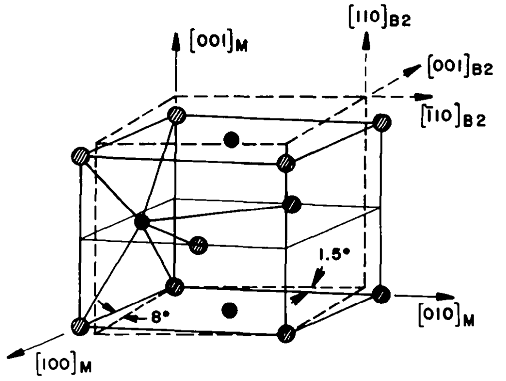

Fig. 2. The orientation relation between the martensite and high-temperature-phase lattice directions. The positions of the atoms after a shuffle of $0{\cdot}06[010]_M$ are indicated.

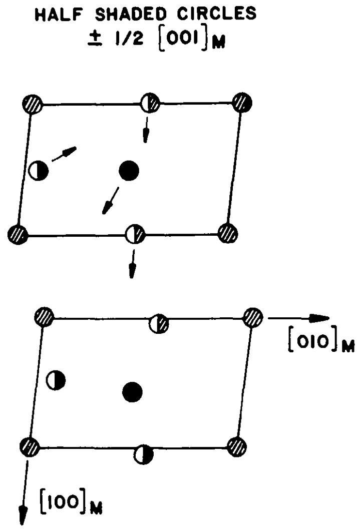

Fig. 3. A projection of the atom positions in the martensite unit cell upon the $(001)_M$ plane showing the atomic movements occurring during the resettling step of the transformation.

Discussion

The agreement between the TiNi powder X-ray data of Wang *et al.* (1972) and the present structure is much better than that of the previous structures. All the calculated and observed peaks agree to within a factor of 0·5 yielding a value of 0·17 for *R* for all 22 peaks. This is a reasonable value considering the accuracy of the data and the fact that no temperature factor was taken into account when the intensities were computed. The relatively high intensity calculated for the $1\bar{1}0$ reflection and appreciable intensities calculated for the 010 and 110 peaks are in agreement with the observed diffraction patterns in Fig. 1(*a*) when the effects of double diffraction are taken into account. The relatively high intensity calculated for the 101 peak is in agreement with the diffraction pattern observed in Fig. 1(*b*). Thus the present structure can account for these two diffraction patterns when double diffraction is considered to be occurring, whereas the previous ones cannot.

Calculated neutron diffraction peak intensities for the present structure are also listed in Table 2, together with experimental values of Wang *et al.* (1972). The negative atomic scattering factor for Ti accentuates the superlattice peaks of the TiNi martensite. There is reasonable matching of the major peaks with those calculated from the present structure. The absence of any observed intensity for the 4·12 Å *d*-spacing reflection from both X-ray and neutron diffraction serves as evidence that the *c* axis of the present structure is indeed the unique axis. The final point supporting the present structure concerns the Ti–Ti bond lengths generated from the final atom positions. The values of around 2·9 Å are consistent with those observed in all the other structures in the Ti–Ni system.

References

DAUTOVICH, D. P. & PURDY, G. R. (1965). *Can. Metall. Q.* **4**, 129–143.

GUPTA, S. P. (1972). *Martensitic Transformation and Stacking Modulations in Titanium–Nickel Alloys of Near-Equiatomic Composition.* PhD Thesis, Polytechnic Institute of Brooklyn.

GUPTA, S. P. & JOHNSON, A. A. (1973). *Trans. Jpn Inst. Met.* **14**, 292–302.

GUPTA, S. P., JOHNSON, A. A. & MUKHERJEE, K. (1973). *Mater. Sci. Eng.* **11**, 29–41.

HEHEMANN, R. F. & SANDROCK, G. D. (1971). *Scr. Metall.* **5**, 801–806.

International Tables for X-ray Crystallography (1968). Vol. III. Birmingham: Kynoch Press.

LARSON, D. J. (1979). *The Physical and Mechanical Properties of Near Equiatomic* TiNi. PhD Thesis, Northwestern Univ.

MARCINKOWSKI, M. J., SASTRI, A. S. & KOSKIMAKI, D. (1968). *Philos. Mag.* **18**, 945–958.

MICHAL, G. M. (1979). *Diffusionless Transformations in* TiNi. PhD Thesis, Stanford Univ.

MOHAMED, H. A. (1976). *Martensitic Transformation and Shape Memory Effect in* Ni–Ti *Alloy.* PhD Thesis, Univ. of California at Berkeley.

MOHAMED, H. A. & WASHBURN, J. (1977). *J. Mater. Sci.* **12**, 469–480.

NAGASAWA, A. (1971). *J. Phys. Soc. Jpn*, **31**, 136–147.

ÖLANDER, A. (1932). *Z. Kristallogr.* **83A**, 145–149.

OTSUKA, K., SAWAMURA, T. & SHIMIZU, T. (1971). *Phys. Status Solidi A*, **5**, 457–470.

SANDROCK, G. D. (1971). *Diffusionless Phase Transitions in Near-Equiatomic Intermetallic Compound Titanium–Nickel.* PhD Thesis, Case Western Reserve Univ.

VATANAYON, S. & HEHEMANN, R. F. (1975). *Shape Memory Effects in Alloys*, edited by A. J. PERKINS, pp. 115–146. New York: Plenum Press.

WANG, F. E., PICKART, S. J. & ALPERIN, H. A. (1972). *J. Appl. Phys.* **43**, 97–112.

ZENER, C. (1947). *Phys. Rev.* **71**, 846–851.

Acta Cryst. (1981). B**37**, 1807–1812

The Structure and Polytypism of the *β* Modification of Copper(I) Thiocyanate*

BY DOUGLAS L. SMITH AND VERNON I. SAUNDERS

Research Laboratories, Eastman Kodak Company, Rochester, New York 14650, *USA*

(*Received* 5 *January* 1981; *accepted* 9 *March* 1981)

Abstract

Crystals of *β*-CuNCS grow as trigonal pyramids. The crystals consist of 3*R* and 2*H* polytypes in syntactic coalescence along with some disorder and twinning. The space groups are *R*3*m* and $P6_3mc$. The lattices have *a* = 3·856 (1) Å. For the 3*R* form, *c* = 16·453 (2) Å, and for 2*H*, *c* = 10·97 Å. The structures are composed of (001) layers of closest-packed cylinders of CuNCS units. As in the case of spheres, there are three possible layer positions called *A*, *B*, and *C* in the *xy* plane. Adjacent layers are bonded to each other by strong Cu–S bonds [2·343 (1) Å] such that both Cu and S are tetrahedrally coordinated and the crystal is a three-dimensional polymer. The structure was solved by inspection and refined to *R* = 0·016 for a strong subset (67 reflections) of the data. Refinement of scale factors for other subsets of the data showed the crystal to be 87% *ABC*, 1% *ACB*, 3% *AB*, and 9% disordered or other polytypes.

Introduction

The reduction of Cu^{II} salts in the presence of thiocyanate ions under various conditions yields at least two polymorphic forms of copper(I) thiocyanate (Kruger, Bussem & Tschirch, 1936; Kruger &

---

* Alternative name: *poly-μ*-(thiocyanato-*N*,*S*)-copper(I).

0567-7408/81/101807-06$01.00